High Rate Photon Irradiation Test of an 8-Plane ATLAS Transition Radiation Tracker Sector Prototype.

Juan Valls
(ATLAS TRT Collaboration)

CERN, 1211 Geneva 23, Switzerland
valls@cern.ch

Abstract

In this document we report the results from a high rate photon irradiation test of an ATLAS Transition Radiation Tracker 8-plane endcap sector prototype with 192 straws instrumented with near to final front-end electronics. Data was taken at the CERN X5 Gamma Irradiation Facility with a ^{137}Cs photon source, and at the Weizmann Institute irradiation facility in Israel with a Gammabeam 150 ^{60}Co source. Results on the performance of the straws are presented in terms of occupancies and noise rates at high counting rates, cross-talk studies between straws, and test pulse hit efficiencies under irradiation.

I. INTRODUCTION

The Transition Radiation Tracker (TRT) detector [1] of the ATLAS experiment at the Large Hadron Collider (LHC) consists of 425,000 straw drift tubes arranged in a central barrel and endcap wheel geometry. The straw walls are surrounded by radiator material for particle tracking and electron identification via Transition Radiation (TR) photons. The straw tubes are 4 mm diameter with a maximum length of 80 cm and operate in the proportional region with a 70% Xe + 20% CF_4 + 10% CO_2 gas mixture and an avalanche gain of $2x10^4$. This allows a prompt collection of prymary electrons and an efficient conversion of the higher energy TR photons through a long term stable operation. To distinguish between TR photons and minimum ionizing particles (MIP) a fast analog shaping combined with two discriminators were implemented in the front-end electronics. A low threshold discriminator allows to detect MIP particles and provides track reconstruction by sampling the signal every 3 ns. A high threshold discriminator allows to identify TR photons.

The TRT has been designed to operate in an extremely high radiation environment. At the expected LHC luminosities of $L = 10^{34}$ cm^{-2} s^{-1} the charged particle and neutron rates in some elements of the detector will approach values of up to 20 MHz. Although the majority of this rate comes from ionizing tracks with average energy depositions in the straws of 2 keV (20 fC equivalent charge), slow neutrons, photons and low momentum charged particles produce signals with energy depositions at the MeV level at a lower rate (several pC equivalent charge). In order to cope with these high occupancies and large variation of energy depositions, the TRT front-end electronics incorporate a precise ion-tail cancellation network in the shaper circuit. Still, large signals or the overlapping ion tails from the pileup of many signals results in a continuous shaper output current with a fluctuating level several times as large as the desired minimum operating threshold. Such a variation of the baseline level introduce an effective spread of discriminator thresholds which leads to the introduction of dead times, loss of efficiency, and a degradation of drift-time resolution and electron identification. With the presence of a differentiating baseline restorer network the sensitivity to this effect is reduced and the efficiency to detect small signals which follow larger ones enhanced.

A study of the straw performance at high counting rates with discrete DC-coupled front-end electronics has already been reported in [2]. The experimental setup for this high rate test consisted on the analog readout of a single wire connected to the anode wire of a straw matrix irradiated by an ^{55}Fe source. Results were given in terms of drift time accuracy and efficiency as a function of counting rate. More recently [3], the same setup was used to characterize a single straw performance with an AC-couple readout through an analog ASDBLR chip with a near to final design.

Here we report on the performance of an endcap TRT 8-plane sector prototype detector exposed to a high radiation photon environment. The 192 straws of the sector prototype were instrumented with the last available front-end electronics. The operation of such a large scale detector prototype is demonstrated by the study of its performance in terms of single channel noise, common mode noise, channel-to-channel cross-talk, recorded occupancies, and single hit detection efficiencies as a function of background counting rate.

II. FRONT-END ELECTRONICS

The front-end electronics of the TRT detector have been designed to best characterize the output signal from the TRT straws. The optimization of the electronic parameters is mainly dictated by the analog signal shape from the straws and the requirement of a reliable and stable operation in a high rate environment. This led to a final design [3] based on a largely differential circuit with a short integration shaping time of 7.5 ns. This value was chosen to optimize tradeoffs between signal to noise and tracking resolution. The circuit includes also a selectable ion-tail compensation network with a capacitively coupled baseline restorer, which allows a compatible operation with Xe or Ar-based gases. Two custom

ASIC's have been developed and implemented in the radiation hard DMILL BiCMOS technology [4]: an 8-channel analog ASDBLR chip and a 16-channel digital DTMROC chip.

The ASDBLR (Amplifier Shaper Discriminator with BaseLine Restoration) provides 8 channels with a preamplifier, shaper, ion tail cancellation, and baseline restorer circuit. The shaper employs the technique of pole-zero cancellation to eliminate the ion tail of the input signal. At the shaper output a baseline restorer is included to eliminate the effects of pileup. The presence of a low and high level discriminator on each channel provides timing signal for tracking and TR photon detection with high efficiency. The low level discriminator has a threshold range of 1 keV (10 fC equivalent input charge), while for the high level discriminator it is 15 keV (150 fC input charge). The output currents from each threshold comparator are summed to provide a ternary encoded output. A low current value (100 μA) indicates a low threshold hit while a higher current output (200 μA) indicates a hit in both discriminators.

The DTMROC (Digital Time Measurement and ReadOut Controller) receives and time-encodes the ADSBLR ternary ouput information from 2 ASDBLR boards (16 channels), stores the data in a memory pipeline and supplies Level 1 formatted data to the back-end electronics. A ternary receiver interprets the output currents from the ASDBLR chips to separate the low and high discriminator levels. The low level discriminator information for each of the 16 channels is digitized in 8 time bins (3.1 ns wide) for each 25 ns beam crossing. This is achieved through an onboard DLL circuit (Delay Locked Loop) which generates 8 LHC 40 MHz clocks with equally phased delays. The high level discriminator information consists only of one bit state, which is added to the track discriminator data to form a 9-bit word. The data is clocked into a pipeline memory and stored until a Level 1 trigger decision arrives. The pipeline depth is 132 locations wide in order to match the 3.3 μs latency of the Level 1 trigger. Upon reception of a trigger the data for 3 time slices is latched into a derandomizer buffer. A readout controller circuit then takes the data and serializes it from the derandomizer to drive it off the chip. The DTMROC provides four 8-bit digital-to-analog converters (DAC) to set the low and high discriminator thresholds of each ASDBLR chip. The threshold for each DAC is common for all 8 channels of the chip. Two test pulse output registers with programmable amplitude and delay are also provided for calibration purposes.

A. Front-End Electronics Characterization

The electrical characterization of the front-end chips was performed with a setup dedicated to TRT system test measurements [5]. The basic parameters to describe the analog chip are the gain, noise, and threshold discriminator offsets and spreads. All measurements have been performed by running the chips at the nominal LHC clock frequency of 40 MHz.

Two different sets of calibration measurements were performed with the chips mounted on the front-end boards: 1) calibration of individual DTMROC chip threshold DAC's, which provides a relationship between DAC counts and voltage at the ASDBLR comparator inputs, and 2) calibration of individual ASDBLR channels, which provide a relationship between an input signal amplitude (either in volts, input charge in fC, or eV energy deposition units) and discriminator threshold (in volts or DAC counts).

1) Digital-toAnalog Converters

The calibration of each of the DTMROC DAC's was done by measuring the output of the discriminator thresholds with a CAMAC voltage ADC module. The average results for each of the four discriminators of the 12 DTMROC chips used in these measurements result in a slope of 5.3 ± 0.1 mV per DAC counts, with an offset of less than 0.5 mV. The DAC output characteristic curve showed also a very good linearity over the entire DAC 8-bit resolution range.

2) Noise, Gain, and Offset Measurements

The gain and offsets for each channel of the analog ASDBLR chip were evaluated by scanning the discriminator thresholds for a given input signal applied externally through injector boards. These boards were specifically designed to mimic the voltage signal shape of point-like ionizations in a TRT straw filled with a Xe-based gas. They were calibrated to provide an output signal of 8.5 mV per 4 keV energy deposited equivalent charge.

For each threshold value a set of pulse signals were applied and the fraction of signals above the discriminator threshold measured. The threshold scan for a given input signal is characterized by an S-curve which is defined as a probability $P(t)$ of surprassing a given threshold t. The signal amplitude corresponds to the threshold equal to the 50% point of the S-curve while the r.m.s. value of the noise can be measured from the width of the S-curve. By measuring the S-curves for different input signal values, the gain of the complete analog circuit after the discriminators and the discriminator input offsets were then extracted.

Figure 1 shows the average gain and offsets for all instrumented channels of the 24 ASDBLR chips used in these measurements. The results are shown for the low and high threshold discriminators respectively. The low threshold discriminator gain and offsets were calculated from measurements taken for input signals between 130 eV and 400 eV. For the high threshold discriminator the input signals were between 2.4 keV and 10 keV. The low threshold average gain is 0.86 mV/eV with a spread of 0.09 mV r.m.s. The high threshold gain is measured to be 0.07 mV/eV with an r.m.s. spread of 0.007 mV. The difference in the gains for the low and high threshold comparators is primarily due to the input attenuator which precedes the comparators. The high threshold discriminator has a 10:1 attenuation at its input with respect the low threshold discriminator. The average discriminator offsets are 122 mV with a r.m.s. spread of 30

mV for the low threshold comparator, and 99 mV with a r.m.s. spread of 27 mV for the high threshold comparator. No significant differences were observed in gain and offsets from chip to chip.

The r.m.s. noise is measured from threshold scans by fitting each single channel S-curve to a complementary error function. The noise level is quite uniform for all connected straws with an average value of 30.8 mV r.m.s. From the average gain of 0.86 mV/eV the noise level is estimated to be 38.5 eV.

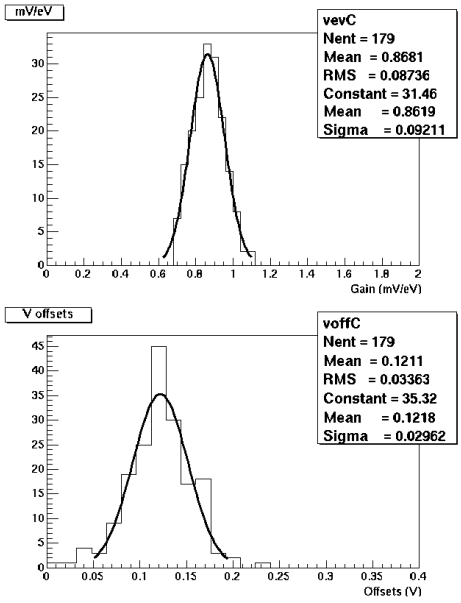

Figure 1: Low threshold dicsriminator gain (mV/eV, top) and offsets (V, bottom).

3) Threshold Spread

The low and high discriminators of each ASDBLR chip share the same threshold for all channels of the chip. This usually leads to offset variations on the thresholds from channel to channel. The design chip objectives for channel to channel offset threshold variation require all offsets to be within 50 eV of a nominal threshold.

III. THE TRT SECTOR PROTOTYPE

The TRT endcap sector prototype consists of 8 planes of 24 straws each with a total of 192 instrumented straws (Figure 2). Each straw is 39 cm long with a 4 mm diameter. Two arc-shaped printed circuit boards (web boards) bring the signals from the straws to the outer radius connectors where the front-end boards with the readout chips are connected. The web board consists of two kapton multi-layers sandwitched between two rigid printed circuit boards. A 50 μm thick kapton single-sided citcuit holds the high voltage traces and petals where the straws are attached while the other board holds the signal circuits. A single HV channel feeds 192 straws through a connection provided on the web boards. A HV line is fed via an input resistor to a group of 8 straws. A signal return lead connects each group of 8 straws through a 1 nF blocking capacitor back to the front-end board and the input of the preamplifiers. The web boards hold the HV decoupling capacitor, the HV isolation resistors, and the input protection circuit of the front-end chips.

Figure 2: ATLAS endcap TRT 8-plane sector prototype.

The smallest endcap TRT readout unit serves 64 straws through separate analog and digital front-end boards. The analog front-end board groups 8 ASDBLR chips. The digital front-end board groups 4 DTMROC chips and connects on top of an ASDBLR board. Three DTMROC boards are then linked through flex kapton cables and interfaced with the back-end electronics through a special cable board.

The active gas in the straws of the sector prototype was a 70% Xe + 20% CF_4 + 10% CO_2 mixture. The detector was operated at a gas flow of 0.08 cm^3/min per straw, which corresponds to about one volume per hour.

IV. IRRADIATION FACILITIES

B. X5 Gamma Irradiation Facility

The Gamma Irradiation Facility (GIF) is a test area placed at the West Area of the CERN SPS where high energy particle detectors are exposed to a particle beam in the presence of a high background flux of photons. These conditions are used to simulate the operation of the detectors at the LHC. The GIF is situated at the downstream end of the X5 test beam. The whole area is surrounded by a concrete wall, 8 m high and 80 cm thick. The GIF provides 662 keV photons produced by a strong radioactive ^{137}Cs source (740 Gbq) which permits to irradiate detectors of up to 6 by 6 m^2 area at 5 meters distance from the source. At 4 meters distance from the source the flux is ~10^5 photons/cm^2/s, with a maximum photon flux of ~10^7 photons/cm^2/s at 1 m where the TRT sector prototype was placed.

C. *Weizmann Institute Irradiation Facility*

The Weizmann Institute irradiation facility in Israel consists of a Gammabeam 150 ^{60}Co source manufactured by MDS Nordion Inc. The ^{60}Co source emits photons of 1173 keV and 1333 keV. The unit consists of a source drawer moving vertically through the center of a cylindrical main shield. With the drawer in the lower vertical position the source is in the center of the main shield. When the drawer is raised the source gets fully exposed above the unit. The source drawer elevation is controlled through a simple motorized pully-cable drive. The Gammabeam 150 ^{60}Co photon source emits a radiation beam 2 inches (5.08 cm) depth at the cylindrical surface of the source, through a 360 degree horizontal arc, and is confined to a 257 degree spherical zone above the top of the surface of the sourcehead.

V. OCCUPANCIES

The different experimental conditions used in this work lead to different background occupancies, counting rates, and energy spectrum shapes. Table 1 shows the different background counting rates corresponding to the different data taking conditions. All values have been calculated for 1 beam crossing. Also shown are the measured counting rates from a single monitoring straw in the web flap with analog readout. The difference in rates as measured with the data and with the monitoring straw arise from different sources: 1) at low counting rates, the rates measured from the data are higher than the measured with the monitoring straw due to a low threshold cross-talk seen in the data from high threshold hits (this cross-talk is not seen in the monitoring straw because straws near it are disconnected; 2) at high counting rates, the rates measured with the monitoring straw are higher than the rates measured from the data due to pile-up events.

LE Occupancy Rate (MHz) LT = 250 eV	HT Occupancy Rate (MHz) HT = 3 keV	Rate in Monitoring Straw (MHz)
1.4 ± 0.8	1.0 ± 0.2	0.5
2.4 ± 1.2	1.6 ± 0.2	1.0
3.6 ± 1.2	3.0 ± 0.5	2.7
5.2 ± 1.4	4.4 ± 1.0	4.7
9.6 ± 2.8	10.3 ± 1.8	9.4
10.5 ± 2.8	13.7 ± 1.9	15.0
12.0 ± 3.4	19.5 ± 3.1	19.0

Table 1: Leading edge and high threshold counting rates (MHz) at different data taking conditions.

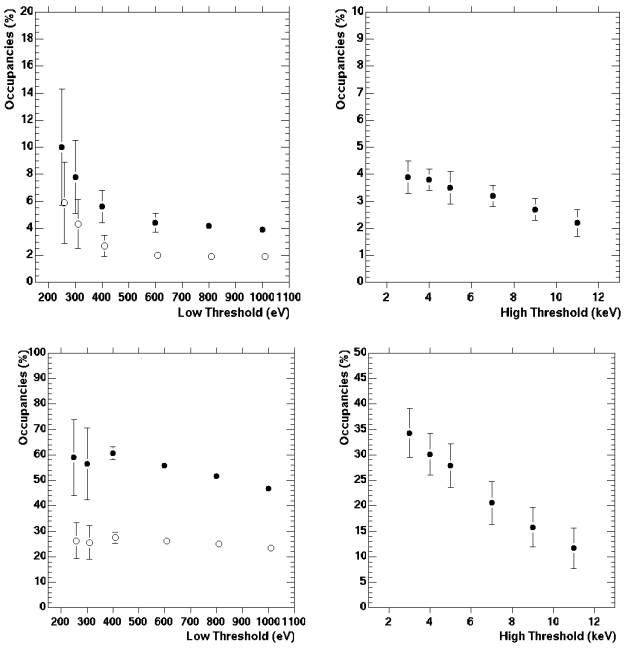

Figure 3: Low threshold (left) and high threshold (right) occupancies (in %) as a function of threshold for 1 MHz (top) and 15 MHz (bottom).

Low and high threshold occupancies as a function of threshold are shown in Figure 3 for two different background counting rates (1 and 15 MHz). Figure 3 suggest a harder energy deposition spectrum shape from high threshold hits for the situations where the sector prototype was placed far away from the photon source and with material in between (low rates). This harder energy spectrum is correlated with the higher low threshold occupancies at low thresholds which is due to cross-talk from high threshold hits.

VI. CROSS-TALK STUDIES

There are two main sources of cross-talk between the straws. First, straws which share the same decoupling capacitor suffer conductive coupling on their signal return. Second, although the straw wall surrounds its wire all over the length of the straw, it is still possible an exposure to the environment at the end of the straw (parasitic capacitive coupling). As 8 straws are connected to a common HV capacitor, one straw will see the cross-talk of the other 7 straws, mainly conductive, when they are fired. The internal channel-to-channel cross-talk of the analog read-out ASDBLR chip is by design less than 0.5%. Finally, the connecting traces on the flex-rigid board as well as the web boards which serve the signals from the straws to the front-end electronics may also contribute to the detected straw-to-straw cross-talk. The effective cross-talk is a superposition of all mentioned coupling paths. Measurements and calculations [6] suggest amplitude cross-talk in the percentage region, but the final cross-talk can reach a manifold of these results

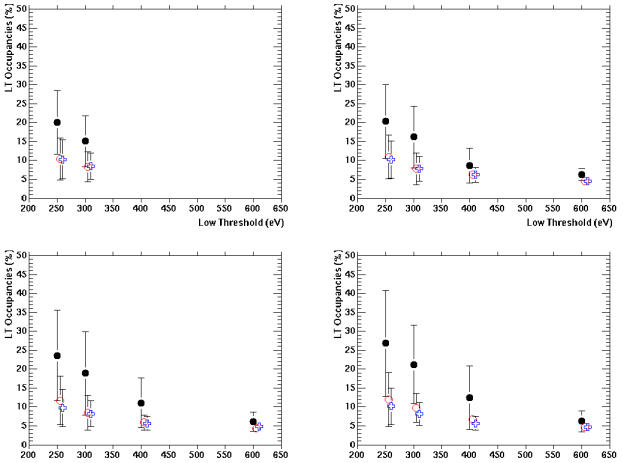

Figure 4: Average low threshold occupancies (%) as a function of low threshold (eV) for a background counting rate of 1 MHz. The different points represent the three sets of straws defined in the text. The trigger straw requires a high threshold hit of 3 (top left), 5 (top right), 9 (bottom, left) and 11 (bottom right) keV.

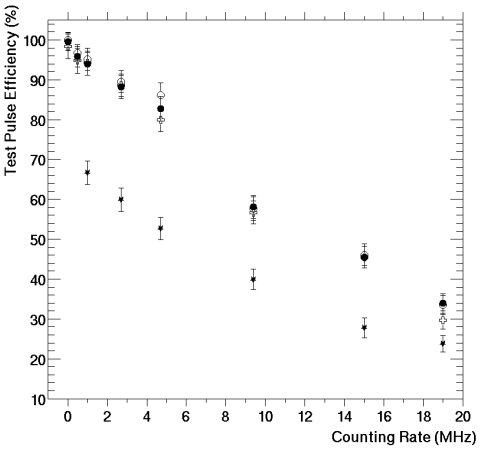

Figure 5: Signal hit efficiencies (%) as a function of background counting rate (MHz) for different low threshold settings (250, 300, 400, and 600 eV). The input test pulse corresponds to 600 eV.

The occupancy cross-talk is studied by calculating occupancies for 3 different sets of straws and for events where only one particular straw is required to contain a hit (at least one high threshold bit set out of the 3 beam crossings). We will refer to this straw as the *trigger straw*. For these events we consider then the average occupancies for the following set of straws: 1) 7 straws sharing the same HV group as the *trigger straw*, 2) 24 straws sharing the same web flap as the *trigger straw* (not included are those straws sharing the same HV group as the *trigger straw*, and 3) 64 straws placed in different web flaps as the *trigger straw*. We refer to these straws as *away straws*. Figure 4 shows the low threshold occupancies as a function of the low threshold for the above defined sets of straws and for a background counting rate of 1.0 MHz. The only significant low threshold occupancy cross-talk observed appears for those straws which share the same HV group as the *trigger straw*. The measurements done at 0.5 and 1.0 MHz show higher cross-talk levels than those obtained at 2.7 MHz. This is mainly due to the different background energy spectrums at these different counting rates. In all cases, the low threshold occupancy cross-talk increases with the high threshold set on the *trigger straw*. For the 0.5 MHz data, the absolute increase in the low threshold occupancies from high threshold hits cross-talk lies between an 11% to 20% for high threshold hits between 5 keV and 11 keV, respectively, and for a 250 eV low threshold. The cross-talk occupancy increase for the 2.7 MHz data lies between a 5% to 10% for high threshold hits between 3 keV and 11 keV, respectively. The difference in the occupancy cross-talk observed at low and high rates is due to the presence of a harder energy spectrum for the high counting rate data taking conditions with respect to the low rate data.

VII. DETECTION EFFICIENCIES

Signal hit detection efficiencies have been measured as a function of background counting rate with calibrated internal test pulses. The hit detection efficiency for a particular channel is defined as the fraction of events with a leading edge hit over the total number of events. A leading edge is always defined as a low to high transition. The internal test pulse signals are adjusted in time to arrive always at the same position at the middle beam crossing. Two different test pulse signals of 15 and 21 DAC's are sent to all channels of all chips. They have been calibrated to provide signals of 600 eV and 1000 eV, respectively. The signal hit efficiencies for different low threshold settings and for the two different test pulses are shown in Figure 5 as a function of the background counting rate. The effect of amplitude pile-up at high rates translates into a decrease of signal efficiency. For a nominal threshold of 250 eV the hit efficiencies decrease from 99.6% to 82.8% at 4.7 MHz counting rates, and from 99.6% to 58.1% at 9.4 MHz for 600 eV signals. For 1000 eV signals the hit efficiencies decrease from 100% to 89.8% at 4.7 MHz and from 100% to 69.7% at 9.4 MHz.

VIII. REFERENCES

[1] ATLAS inner detector technical design report, CERN/LHCC/97-17, ATLAS TDR 5, 30 April 1997.

[2] T. Akesson et al., Nucl. Instr. And Meth. A 367 (1995) 143.

[3] T. Akesson at al., Nucl. Instr. And Meth. A 449 (2000) 446.

[4] B. Bevensee et al., IEEE Trans. Nucl. Sci. NS-43 (N3) (1996) 1725.

[5] A. Romaniouk, J. Valls, *GIF Irradiation Tests with an 8-Plane TRT Endcap Sector Prototype*, ATLAS Internal Note, ATL-INDET-2002-018; A. Romaniouk, J. Valls, *High Rate Photon Irradiation Test of an Endcap TRT Sector Prototype*, ATLAS Internal Note, ATL-INDET-2002-019; J. Valls, *XTRT – A Program for TRT System Tests*, ATLAS Internal Note, ATL-INDET-2002-020.

[6] P. Lichard, private communication.